Energy Efficiency Oriented Cross-Layer Resource Allocation for Multiuser Full-Duplex Decode-and-Forward Indoor Relay Systems at 60 GHz

Zhongxiang Wei, *Student Member, IEEE,* Xu Zhu, *Senior Member, IEEE,* Sumei Sun, *Fellow, IEEE,* and Yi Huang, *Senior Member, IEEE*

***Abstract*—Energy efficiency (EE)-oriented green communication design is an important issue at 60 GHz due to high power consumption of devices working at such high frequency. In this paper, we investigate EE-oriented resource allocation for full-duplex (FD) decode-of-forward (DF) relay-assisted 60 GHz multiuser indoor systems. In contrast to the existing spectral efficiency (SE)-oriented designs, our scheme maximizes EE for FD relaying system under cross-layer constraints, addressing the typical problems at 60 GHz, such as the intermittent signal blockage caused by the small wavelength of millimeter (mm)-wave. A low-complexity EE-orientated resource allocation algorithm is proposed, by which the transmission power allocation, subcarrier allocation and throughput assignment are performed jointly across multiple users. Simulation results verify our analytical results and confirm that the FD relaying with the proposed algorithm achieves a higher EE than the FD relaying with SE-oriented approaches, while offering a comparable SE. In addition, a much lower throughput outage probability is guaranteed by the proposed resource allocation algorithm, showing its robustness against channel estimation errors. A full range of power consumption sources and imperfect self-interference cancellation are considered to rationalize our analysis.**

***Index Terms*—Energy efficiency, full-duplex, cross-layer, resource allocation, decode-and-forward relay, 60 GHz**

I. Introduction

Communication at 60 GHz, referred to as millimeter (mm)-wave communication, has attracted much attention, as the precedented $3-9$ GHz bandwidth of 60 GHz enables multi-Gbps transmission and supports much richer multi-media services in short range communication scenario. Two fundamental distinguishing features of 60 GHz are the high propagation loss (PL) and blockage impact [1], *e.g.,* the PL at 60 GHz is 28 dB higher than that at 2.4 GHz and 20 dB higher than that at 5 GHz. Therefore, relaying technique is a leverage to extend network coverage and maintain network connectivity at 60 GHz [2]. Relaying techniques can be classified as either half-duplex (HD) or full-duplex (FD). FD relay receives and transmits simultaneously on the same frequency and therefore has potentiality on high-speed transmission, enhancing the system spectrum efficiency (SE). However, FD operation suffers self-interference and requires effective self-interference mitigation [3]. On the other hand, the escalation of energy consumption at 60 GHz has been recognized as a major threat to environmental protection. This is because 60 GHz chips generally consume much more power than the chips working at a much lower frequency [4], and more power is needed by FD relays due to the self-interference cancellation operation [2]. Therefore, green communication design, which is energy efficiency (EE)-oriented, is important for 60 GHz FD relaying communications.

Thanks to recent advances in self-interference cancellation technologies [3] [5] [6] [7], FD relaying becomes feasible in practice, where the strong self-interference can be mitigated effectively. There are three main methods to suppress self-interference at relay node: passive suppression (PS), analog cancellation (AC) and digital cancellation (DC) [3]. The first stage of self-interference cancellation, PS, mitigates self-interference in the propagation domain, which benefits from directional antenna, antenna placement and antenna shielding [5]. After PS, self-interference can be further mitigated by AC before signal goes through low noise amplifiers [6]. The last stage, DC is applied in digital domain, which subtracts the residual self-interference after PS and AC in digital domain [7]. Up to 100 dB of cancellation amount can be achieved by existing methods [3] [8]. With recent advances in self-interference cancellation and hardware designs, FD is also considered in mm-wave communications for high-speed and low-latency transmission. A 60 GHz transceiver with FD fiber-optic transmit and receive chains was developed for short-range broadband application in [9], while [10] [11] explored the FD implementation in mm/sub-mm wave Si-constructed chips. The authors in [12] studied the self-interference cancellation in mm-wave FD systems. It has been found that, combined with PS, AC and DC, as much as $80-100$ dB self-interference cancellation amount can be achieved in both line-of-sight (LOS) and non-LOS (NLOS). Also, benefiting from mm-wave transmission, PS at 60 GHz can be naturally higher than that at lower frequency, *e.g.*, 2.4/5 GHz, which was also featured in [2]. Addressing the excessively high PL and sensitivity to blockage, the authors in [13] designed a transmit

Manuscript received January 31, 2016; revised May 15, 2016; accepted August 06, 2016. Date of publication December, 2016; date of current version August 15, 2016. This work was supported by the University of Liverpool and A*STAR.

Zhongxiang Wei, Xu Zhu and Yi Huang are with the Department of Electrical Engineering and Electronics, the University of Liverpool, Liverpool, L69 3GJ, UK, (email: {hszwei,xuzhu}@liverpool.ac.uk).

Sumei Sun is with the Institute for Infocom Research, A*STAR, Singapore, 138632, Singapore.

and receive beamforming scheme for FD transmission at mm-wave frequency, obtaining a higher degrees of freedom (and therefore higher SE) compared to HD.

Much research has been conducted on optimal resource allocation for FD transmission in terms of maximizing SE. In [14], [15] and [16], SE maximization was investigated in bi-directional FD networks. In [14], the optimal transmission power policies at two communicating nodes were proposed to maximize ergodic capacity in a FD multi-input-multi-output (MIMO) communication system. In [15], a beamforming scheme was proposed to maximize SE in small cell networks, where a FD base station (BS) communicates with multiple HD users in the uplink and downlink channels simultaneously. In [16], the authors considered a single cell FD orthogonal frequency division multiple access (OFDMA) network, which consists of one FD BS and multiple FD users. The subcarrier and power allocation were jointly optimized in terms of sum-capacity. While in [17] [18] [19] and [20], SE maximization of FD relay-assisted networks was investigated. In [17], a joint relay selection and power allocation method for maximizing signal-to-interference-and-noise-ratio (SINR) was proposed in a multiple amplify-and-forward (AF) FD relay system. In [18], a joint precoding/decoding design was presented to maximize end-to-end SINR in an AF FD relay network. In [19], the combination of opportunistic relay mode selection and transmit power adaptation at source was proposed to maximize SE. While in [20], resource allocation issue in multiuser MIMO networks was investigated in terms of SE. FD transmission in cognitive radio (CR) networks was researched in [21] and [22], respectively. Based on time division multiplex access (TDMA) (therefore HD transmission), the authors in [23] [24] studied the SE maximization in 60 GHz wireless personal area networks.

In terms of EE-oriented resource allocation, all existing work has focused on HD relaying [25] [26] [27] [28] or direct transmission (without relay) [29] [30] [31] [32]. In [25], maximizing EE was investigated for MIMO OFDMA based Long Term Evolution (LTE) cellular systems. While in [26], a power consumption model was presented for HD relay-assisted 60 GHz systems. However, it did not consider FD mode nor static circuit power, which is actually comparable with the transmission power in indoor environments. The authors of [27] studied the EE-SE trade-off in a multiuser cellular virtual-MIMO system with decode-and-forward (DF) type protocols, however, only transmission power was considered as power consumption. In [28], the position of HD relay was investigated to outperform direct (without relay) transmission in terms of EE. In [29], EE issue was researched for MIMO-orthogonal frequency division multiple (OFDM) systems with statistical quality-of-service (QoS) constraints, where only transmission power was considered. EE-oriented resource allocation of OFDMA networks in downlink was considered in [30] [31] [32]. The authors indicated that transmission power and circuit power need to be considered together to rationalize the power consumption model. Besides, EE-oriented designs in CR networks were given in [22] and [33]. In [34], the authors investigated the EE balance between downlink and uplink transmission in a single cell system, where a base station can communicate with users via time division duplex (TDD) transmission mode. Since uplink and downlink transmission were decoupled in orthogonal time slots, the self-interference can be avoided at the expense of SE. In [35], the EE-oriented resource allocation was investigated in heterogeneous networks with multiple access points, in which the multi-objective optimization problem was transformed into an equivalent single objective optimization problem by the weighted Tchebycheff method to find the Pareto optimal solution. Resource allocation for uplink in LTE networks was investigated in [36]. However, the authors took maximization of total uplink SE as objective function. Therefore, the EE may not be optimal due to the fully utilized transmission power. In [37], the EE-oriented resource allocation was investigated for uplink of LTE networks under QoS requirements. However, only transmission power was taken into account to trace the total power consumption. In [38], the power consumption model was investigated for LTE based marco/pico cell, revealing that MIMO may not lead to energy saving due to the increased circuit power consumption. Also, EE issues in 5G systems were extensively reviewed in [39], and a variety of EE optimization methods in uplink and downlink were discussed.

The aforementioned EE-oriented resource allocation methods designed for HD relaying or direct transmission may not be directly applied to FD relaying systems due to the presence of residual self-interference, while most existing work on resource allocation for FD relaying systems was presented to maximize SE. On the other hand, due to the significant PL of mm-wave communications, ultra-dense small cell network and WiFi access points are promising solutions for local-area connectivity, which act as front/back haul to provide seamless coverage in 5G systems [40]. The application of small cell network was presented in [41] [42] for indoor/outdoor use. It was also indicated that relay-assisted optimal resource allocation in mm-wave small cell is still challenging. The EE issue of FD transmission was investigated in our previous work [2]. However, it focused on the comparison between HD and FD with different self-interference cancellation schemes in a single user AF relay system, and also did not consider cross-layer design and multiuser scenarios. In [43], EE-oriented resource allocation in cellular networks with FD relaying was investigated. However, only physical layer (PHY) resource allocation was considered. Besides, the FD relaying power consumption model in [43] is not accurate since the power consumption for self-interference cancellation at FD relay was ignored. There lacks investigation of cross-layer EE-oriented resource allocation for multiuser FD relaying in the literature, which is the motivation of our work.

In this paper, we investigate cross-layer EE-oriented resource allocation for multiuser FD DF relay-assisted indoor systems, which is the first work to the best of our knowledge. Our work is different in the following aspects.

1. To address cross-layer design for FD relaying system at 60 GHz, throughput outage probability, a media access control (MAC) layer performance metric, is considered, while only PHY layer performance metrics were considered in our previous work [2]. This makes the proposed work more practical at 60 GHz than existing resource allocation works

[7] [20] [43] [44], since throughput outage easily occurs in the presence of channel estimation errors and out-of-date channel state information (CSI), caused by mobility of users and intermittent blockage effects at 60 GHz.

2. A low-complexity resource allocation algorithm, referred to as the Q-FERA algorithm, is proposed, by which the transmission power, subcarrier and throughput are allocated jointly across multiple users to maximize system EE. Based on the proposed EE-oriented resource allocation algorithm, FD relaying can achieve a higher EE than FD relaying with an SE-oriented approach in [20], while offering a comparable SE. In addition, the throughput outage probability is much lower by the proposed Q-FERA algorithm, showing its robustness against the channel estimation errors.

3. Properties of the EE-oriented resource allocation are investigated: 1) Impact of transmission power on EE is investigated, revealing that utilizing higher transmission power does not ensure a higher EE. Especially, higher transmission power at relay node may degrade both EE and SE, with poor self-interference cancellation performance. 2) EE-oriented water-filling for two-hop FD relaying is presented, which indicates that more power will be allocated to the subcarriers with lower residual self-interference. 3) By trading off SE and EE in FD relaying systems, FD relaying with the proposed Q-FERA algorithm can outperform FD relaying with SE-oriented algorithms in terms of EE, at the expense of SE. 4) With a higher Rician factor (indoor 60 GHz channel can be modeled by Rician fading with a typical Rician factor of $5-15$ dB), more aggressive throughput can be assigned while satisfying the target outage probability, which reflects the suitability of the proposed algorithm for 60 GHz. 5) Impact of outage probability constraint on EE is researched, showing that adopting stringent outage probability constraint does not necessarily guarantee a higher EE.

In Section II, the system model and problem formulation are presented. Analysis of throughput and power consumption is given in Section III. EE-oriented cross-layer resource allocation design is presented in Section IV and complexity analysis is given in Section V. Numerical results and conclusions are shown in Sections VI and VII, respectively.

II. SYSTEM MODEL AND PROBLEM FORMULATION

In this section, we describe the system model in Subsection II-A, and then present the optimization problem in Subsection II-B.

A. System Model

We consider a K-user FD DF relay-assisted system in the downlink, as illustrated in Fig. 1. It is assumed that the users can not hear the source directly [23]. This typical assumption corresponds to coverage extension scenarios due to high attenuation at 60 GHz [2]. The relay works in FD mode, causing self-interference to the receiver from its transmitter. Self-interference cancellation schemes, PS, AC and DC are applied at the relay, as shown in Fig. 1.

We assume OFDMA transmission with N subcarriers. Let $h_{SR,k,n}$, $h_{RD,k,n}$ and $h_{RR,k,n}$ denote the channel frequency responses of links source-to-relay (S-R), relay-to-user (R-D) and relay-to-relay (R-R) on subcarrier n for user k, respectively. Also let $l_{SR,k}$, $l_{RD,k}$ and $l_{RR,k}$ denote the PLs of links S-R, R-D and R-R for user k, respectively. The channels of the S-R and R-D links are modeled as Rician fading [45], which is widely used for 60 GHz channel modeling [46] [47]. Without loss of generality, we assume that the Rician factor $\hat{k}$ is equal at the two links, *i.e.,* $h_{SR,k,n} \sim CN(\sqrt{\hat{k}/(1+\hat{k})}, 1/(1+\hat{k}))$ and $h_{RD,k,n} \sim CN(\sqrt{\hat{k}/(1+\hat{k})}, 1/(1+\hat{k}))$. Normally, the Rician factor $\hat{k}$ varies between 5 dB and 15 dB in 60 GHz indoor environment [45]. The self-interference channel is modeled as Rayleigh fading channel as the LOS between the transmitter and the receiver of the relay can be effectively blocked by antenna shielding and placement due to the very small wavelength at 60 GHz [2]. The self-interference waves are collected from reflected waves [48]. We assume that perfect CSI of link S-R can be obtained. Since both the BS and relay are static and fixed high in indoor environment and is immune to the blockage effect, the fading gain can be reliably estimated with negligible estimation error [49], whereas the channel estimation error of the link R-D is presented with imperfect channel estimate $h_{\hat{RD},k,n}$ and estimation error $\Delta h_{RD,k,n} \sim CN(0, \sigma^2_{error})$, where σ^2_{error} is the variance of the estimation error and is independent of k and n. It is because the wavelength at 60 GHz is only 5 mm, any obstacles whose size is significant larger than the wavelength will cause serious blockage effect [50], *e.g.,* mobility of human or small-size furniture can even eliminate the LOS transmission and penalize the link by $20-30$ dB, resulting in time-varying channel state and out-of-date CSI of link R-D. Besides, the channel estimation error of link R-R is absorbed into the effect of cancellation amount α [2], *i.e.,* higher value of α means more accurate estimation of link R-R and lower circuit distortion of the self-interference cancellation operation [1].

For OFDMA usage in multiuser scenario, define power allocation matrices $\boldsymbol{P_s} = [p_{s,k,n}]_{K\times N}$, $\boldsymbol{P_r} = [p_{r,k,n}]_{K\times N}$, whose elements $p_{s,k,n}$ and $p_{r,k,n}$ denote the transmission powers allocated at the resource and the relay node for user k on subcarrier n, respectively. Define subcarrier allocation matrix $\boldsymbol{\rho} = [\rho_{k,n}]_{K\times N}$, whose element $\rho_{k,n} = \{1, 0\}$ denotes whether subcarrier n is assigned to user k (by 1) or not (by 0). Subcarrier mapping is not considered due to high complexity. $z_{R,k,n}[i]$ and $z_{D,k,n}[i]$ denote complex Additive White Gaussian Noise (AWGN) on subcarrier n introduced at the relay and user k in time slot i, respectively, with zero mean and variance σ^2. Define end-to-end instantaneous capacity matrix $\boldsymbol{C} = [c_{k,n}]_{K\times N}$, whose element $c_{k,n}$ denotes end-to-end capacity of user k achieved on subcarrier n, and overall capacity is calculated as $C = \sum_{k=1}^{K}\sum_{n=1}^{N} c_{k,n}$. In

[1]There are other models which assume that the residual self-interference is proportional to the transmission power [44], or the residual self-interference increases the noise power by a coefficient σ regardless of the transmission power [16]. The first modeling of self-interference actually is the same method as we formulated, since the self-interference is the transmitted signal from the relay node itself and the power of residual self-interference is directly determined by the relay's transmission power and the self-interference cancellation amount α. While the second one simplifies the self-interference model by ignoring the transmission power at the transmitter.

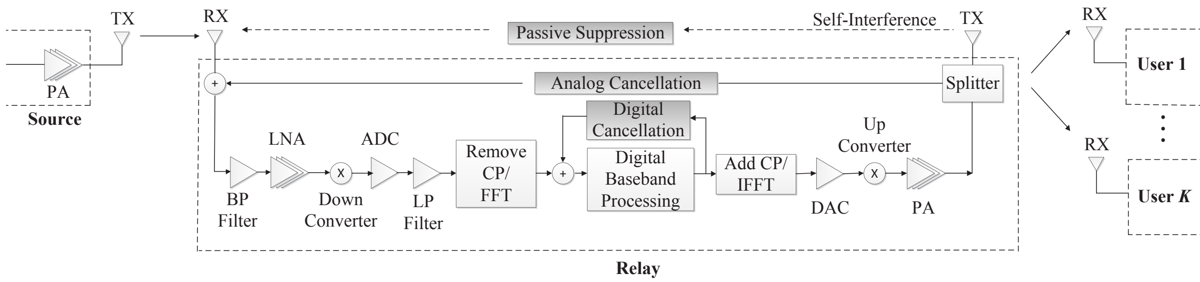

Fig. 1. Simplified FD DF relay assisted system in the downlink, with PS, AC and DC of self-interference cancellation.

most cross-layer designs, capacity is a meaningful measure when the schedulers have perfect CSI. However, in practice, outage occurs whenever throughput exceeds the instantaneous capacity, which is caused by the channel estimation error [49]. Therefore, the per-subcarrier outage constraint is needed to ensure low frame error rate applications [51] and to avoid network congestion caused by the retransmission of lost message. Therefore, we define the instantaneous throughput $t_{k,n}$ of user k on subcarrier n, given by

$$t_{k,n} = \begin{cases} t_{k,n}, t_{k,n} \leq c_{k,n} \\ \;0\;, t_{k,n} > c_{k,n}. \end{cases} \tag{1}$$

Denote $\boldsymbol{T} = [t_{k,n}]_{K\times N}$ as the throughput assignment policy and the overall throughput of system is calculated as $T = \sum_{k=1}^{K}\sum_{n=1}^{N} t_{k,n}$.

B. Problem Formulation

Define $\eta(\boldsymbol{\rho}, \boldsymbol{P_s}, \boldsymbol{P_r}, \boldsymbol{T})$ as the EE (in bits/Joule), which is the ratio of the system throughput T to the incurred total power consumption P_{total}. Accordingly, the optimal EE resource allocation problem of the FD DF relaying system is formulated as

$$P1: \underset{\boldsymbol{\rho}, \boldsymbol{P_s}, \boldsymbol{P_r}, \boldsymbol{T}}{\operatorname{argmax}} \; \eta(\boldsymbol{\rho}, \boldsymbol{P_s}, \boldsymbol{P_r}, \boldsymbol{T}) = \frac{T}{P_{total}}, \tag{2}$$

$s.t.$ $(C1): \sum_{k=1}^{K}\sum_{n=1}^{N}(p_{s,k,n} + p_{r,k,n}) \leq P_{max}$, $(C2): p_{s,k,n} \geq 0,\; p_{r,k,n} \geq 0$, $(C3): \sum_{k=1}^{K}\rho_{k,n} = 1$, $(C4): \rho_{k,n} \in \{0,1\}$, and $(C5): Pr[t_{k,n} > c_{k,n} \mid \hat{h}_{RD,k,n}] \leq \theta^k$ for $\forall k \in K$ and $n \in N$, where $(C1)$ is a joint power constraint for the source and relay with a maximum total transmission power P_{max}, which provides useful insight into the power usage of the whole system rather than the per-hop required power [49]; $(C2)$ implies non-negative transmission power allocation at the source and relay; $(C3)$ and $(C4)$ are imposed to guarantee that each subcarrier is only used by one user; $(C5)$ represents a per-subcarrier throughput outage probability constraint for user k on subcarrier n with the estimated channel $\hat{h}_{RD,k,n}$, *i.e.*, the probability that the assigned throughput $t_{k,n}$ on subcarrier n exceeds its channel capacity $c_{k,n}$ is upper bounded by θ^k. $(C1)-(C4)$ are PHY constraints while $(C5)$ is a MAC layer constraint.

III. Throughput and Power Consumption Analysis

The problem formulation in (2) includes the system throughput and total power consumption. Hereby, we analyze the throughput and power consumption in Section III. At the relay node, the received signal for user k on subcarrier n in time slot i is

$$r_{k,n}[i] = h_{SR,k,n}\sqrt{l_{SR,k}p_{s,k,n}}x_{k,n}[i] + h_{RR,k,n}\sqrt{\frac{l_{RR,k}}{\alpha}}q_{k,n}[i] + z_{R,k,n}[i], \tag{3}$$

where $x_{k,n}[i]$ is the transmitted signal from the source on subcarrier n for user k in time slot i. The DF relay decodes the received signal and re-encodes and forwards it to user k. Therefore, the transmitted signal $q_{k,n}[i]$ from the relay for user k on subcarrier n is given by

$$q_{k,n}[i] = \sqrt{p_{r,k,n}}x_{k,n}[i-\tau], \tag{4}$$

where the integer $\tau \geq 1$ is the symbol delay. At the user end, the received signal is

$$y_{k,n}[i] = h_{RD,k,n}\sqrt{l_{RD,k}p_{r,k,n}}x_{k,n}[i-\tau] + z_{D,k,n}[i]. \tag{5}$$

Therefore, the SINRs at the first hop S-R and the second hop R-D are given by (6) and (7), respectively.

$$\Gamma_{1,k,n}^{FD} = \frac{p_{s,k,n}\gamma_{SR,k,n}}{1 + p_{r,k,n}\gamma_{RR,k,n}}, \tag{6}$$

$$\Gamma_{2,k,n}^{FD} = p_{r,k,n}\gamma_{RD,k,n}, \tag{7}$$

where $\gamma_{SR,k,n} = \frac{h_{SR,k,n}^2 l_{SR,k}}{\sigma^2}$, $\gamma_{RD,k,n} = \frac{h_{RD,k,n}^2 l_{RD,k}}{\sigma^2}$ and $\gamma_{RR,k,n} = \frac{h_{RR,k,n}^2 l_{RR,k}}{\alpha\sigma^2}$ are channel-to-noise ratios (CNRs) of links S-R, R-D and R-R, respectively. For the FD DF relaying system, the end-to-end capacity on subcarrier n for user k is given by

$$c_{k,n} = \rho_{k,n} min\{log_2(1 + \Gamma_{1,k,n}^{FD}), log_2(1 + \Gamma_{2,k,n}^{FD})\}. \tag{8}$$

On the other hand, for short-range communications, the power amplifier (PA) power is comparable with the circuit power [30] due to the small chip size in indoor environment and the low drain efficiency of 60 GHz chips [52], and is given by

$$P_{PA}=\frac{1}{\omega}\sum_{k=1}^{K}\sum_{n=1}^{N}(p_{s,k,n}+p_{r,k,n}), \tag{9}$$

where ω is the drain efficiency. The circuit power includes the power consumed by all circuit blocks along the signal path, which can be divided into static circuit power, $P_{c,sta}$, and dynamic circuit power, $P_{c,dyn}$ [30]. A well-accepted model of dynamic circuit power is $P_{c,dyn}=\varepsilon T$, where the constant ε denotes the power consumption per unit data rate.

For FD relay, applying PS actually does not consume additional power, however, the power consumed by AC and DC is non-negligible. Besides, the power consumed by the involved chip components, such as attenuator, splitter and adder are not related to the throughput state [3], and therefore the power consumed by AC and DC, P_{AD}, is regarded as a constant. The total power consumption of FD relaying system is formulated as

$$P_{total}=\underbrace{\frac{1}{\omega}\sum_{k=1}^{K}\sum_{n=1}^{N}(p_{s,k,n}+p_{r,k,n})}_{\text{PA power}}+\underbrace{P_{c,sta}+\varepsilon T}_{\text{circuit power}}+P_{AD}. \tag{10}$$

IV. Energy Efficient Cross-Layer Resource Allocation

Based on the derived throughput and total power consumption in Section III, substituting (1), (8) and (10) into (2) yields the EE-oriented resource allocation problem of the FD DF relaying system:

$$P2:$$
$$\underset{\boldsymbol{\rho},\boldsymbol{P_s},\boldsymbol{P_r},\boldsymbol{T}}{\operatorname{argmax}}\ \frac{T}{\frac{\sum_{k=1}^{K}\sum_{n=1}^{N}(p_{s,k,n}+p_{r,k,n})}{\omega}+P_{c,sta}+\varepsilon T+P_{AD}}, \tag{11}$$

$s.t.\ (C1)-(C5)$.

The policies of subcarrier allocation $\boldsymbol{\rho}$, transmission power allocation $\boldsymbol{P_s}$ and $\boldsymbol{P_r}$ and throughput assignment $\boldsymbol{T}$ need to be optimized jointly, subject to the cross-layer constraints. To solve the non-convex problem P2 in a polynomial time, a series of transformations are needed, *i.e.,* solving the original P2 is transformed into solving P3 and P4, as presented in Subsection IV-A. Final solution is demonstrated in Subsection IV-B, and discussion of EE-oriented design is given in Subsection IV-C.

A. Transformations of the Optimization Problem

We first introduce a new variable to combine $\boldsymbol{P_s}=[p_{s,k,n}]_{K\times N}$ and $\boldsymbol{P_r}=[p_{r,k,n}]_{K\times N}$ without the loss of optimality [20]. Let matrix $\boldsymbol{P}=[p_{k,n}]_{K\times N}$ denote end-to-end transmission power policy, whose element $p_{k,n}=p_{s,k,n}+p_{r,k,n}$ represents end-to-end transmission power for user k on subcarrier n via hops S-R and R-D. For DF relaying, the maximum EE for user k on subcarrier n is achieved when $\Gamma_{1,k,n}^{FD}=\Gamma_{2,k,n}^{FD}$ (which is easy to prove by a counter example). Let $p_{r,k,n}=p_{k,n}-p_{s,k,n}$ and substitute it into $\Gamma_{1,k,n}^{FD}=\Gamma_{2,k,n}^{FD}$. We can solve the quadratic function of $p_{r,k,n}$ and equivalent end-to-end capacity $c_{k,n}$ of FD DF relaying on subcarrier n for user k is given by Lemma 1.

Lemma 1: The equivalent end-to-end capacity of FD DF relaying for user k on subcarrier n is given by (12).

Next we need to incorporate the MAC layer constraint in $(C5)$ with the PHY layer parameters. The "$\leq$" sign in $(C5)$ is replaced with an "$=$" sign, which is reasonable in low outage probability applications (*e.g.*, $\theta^k\leq$0.01) [49]. The equivalent outage probability constraint is given by Lemma 2.

Lemma 2: The outage probability constraint in $(C5)$: $Pr[t_{k,n}>c_{k,n}\mid h_{R\hat{D},k,n}]=\theta^k$ for $\forall k\in K$ and $n\in N$, is equivalent to allocating throughput as

$$t_{k,n}=log_2(1+\Lambda_{k,n}), \tag{13}$$

where $\Lambda_{k,n}=\frac{\sqrt{4p_{k,n}\Phi_{k,n}+\Psi^2}-\Psi}{2\gamma_{RR,k,n}}$, $\Psi_{k,n}=\gamma_{R\hat{D},k,n}+\gamma_{SR,k,n}$, $\Phi_{k,n}=\gamma_{R\hat{D},k,n}\gamma_{SR,k,n}\gamma_{RR,k,n}$ and $\gamma_{R\hat{D},k,n}=\frac{F_{k,n}^{-1}(\theta^k)\sigma_{error}^2 l_{RD,k}}{2\sigma^2}$. $F_{k,n}(\cdot)$ denotes the cumulative distribution function (cdf) of the non-central chi-square random variable, with 2 degrees of freedom, and non-central parameter $\frac{2|h_{R\hat{D},k,n}|^2}{\sigma_{error}^2}$. $F_{k,n}^{-1}(\cdot)$ denotes the inverse function of $F_{k,n}(\cdot)$.

Proof: See Appendix A.

We then relax the combinational constraint $(C4)$ caused by the subcarrier assignment. The binary variable $\rho_{k.n}$ is relaxed to a real number within the interval [0,1], indicating the time sharing factor of subcarrier n among K users. The relaxation of $(C4)$ does not affect the optimality when the number of subcarriers goes to infinity ($N\to\infty$). Given a large number of subcarriers, the loss of optimality is negligible and the solution after relaxation is near-optimal [53]. Hence, the transformed problem P3 is given by (14).

Notice that $(C1)$ and $(C4)$ are transformed to $(C7)$ and $(C6)$, respectively, whereas $(C5)$ can be omitted after the transform through Lemma 2. Therefore, optimizing $\eta(\boldsymbol{\rho},\boldsymbol{P_s},\boldsymbol{P_r},\boldsymbol{T})$ under constraints $(C1)-(C5)$ is transformed into optimizing $\eta(\boldsymbol{\rho},\boldsymbol{P})$ under new constraints $(C2)$ $(C3)$ $(C6)$ and $(C7)$ through Lemmas 1 and 2. We now introduce Theorem 1 to help solve the problem P3.

Theorem 1: EE $\eta(\boldsymbol{\rho},\boldsymbol{P})$ is strictly quasi-concave or mono-increasing with respect to the total end-to-end transmission power P, under a maximum transmission power constraint P_{max}.

Proof: See Appendix B.

Theorem 1 confirms the existence and uniqueness of the global maximum $\eta(\boldsymbol{\rho},\boldsymbol{P})$. Obviously, the target function EE $\eta(\boldsymbol{\rho},\boldsymbol{P})$ is mono-increasing with respect to the total end-to-end throughput T with a fixed end-to-end transmission power P. According to Theorem 1, if there is a globally optimal end-to-end transmission power P^*, maximizing $\eta(\boldsymbol{\rho},\boldsymbol{P})$ is equal to maximizing the total end-to-end throughput with this P^* rather than P_{max}. Then the optimization problem P3 in (14) can be transformed into

$$P4:\underset{\boldsymbol{\rho},\boldsymbol{P}}{\operatorname{argmax}}\sum_{k=1}^{K}(1-\theta^k)\sum_{n=1}^{N}\rho_{k,n}log_2(1+\frac{\Lambda_{k,n}}{\rho_{k,n}}), \tag{15}$$

$$c_{k,n}=\rho_{k,n}log_2\big(1+\frac{\sqrt{4p_{k,n}\gamma_{RD,k,n}\gamma_{SR,k,n}\gamma_{RR,k,n}+(\gamma_{RD,k,n}+\gamma_{SR,k,n})^2}-(\gamma_{RD,k,n}+\gamma_{SR,k,n})}{2\gamma_{RR,k,n}}\big). \tag{12}$$

$$P3:\underset{\boldsymbol{\rho},\boldsymbol{P}}{\mathrm{argmax}}\frac{\sum_{k=1}^{K}(1-\theta^k)\sum_{n=1}^{N}\rho_{k,n}log_2(1+\frac{\Lambda_{k,n}}{\rho_{k,n}})}{\frac{\sum_{k=1}^{K}\sum_{n=1}^{N}p_{k,n}}{\omega}+P_{c,sta}+\varepsilon\sum_{k=1}^{K}(1-\theta^k)\sum_{n=1}^{N}\rho_{k,n}log_2(1+\frac{\Lambda_{k,n}}{\rho_{k,n}})+P_{AD}}, \tag{14}$$

$$s.t.\ (C2),\ (C3),\ (C6){:}\ \rho_{k,n}\in[0,1]\text{ and }(C7){:}\ \sum_{k=1}^{K}\sum_{n=1}^{N}p_{k,n}\leq P_{max}.$$

$s.t.$ $(C2)$, $(C3)$, $(C6)$ and $(C8)$: $\sum_{k=1}^{K}\sum_{n=1}^{N}p_{k,n}=P^*$, where $(C8)$ is a transform of $(C7)$ according to Theorem 1. Notice that P_{max} is replaced by P^* in $(C8)$.

B. Solution to the Cross-Layer Resource Allocation Algorithm

After a series of transformations in Subsection IV-A, the problem P4 in (15) is jointly-concave in terms of $p_{k,n}$ and $\rho_{k,n}$, which is proved in Appendix C. To solve the problem P4, Lagrange multiplier method [54] is applied. The Lagrange function of (15) is given by

$$\begin{aligned}L=&\sum_{k=1}^{K}(1-\theta^k)\sum_{n=1}^{N}\rho_{k,n}log_2(1+\frac{\Lambda_{k,n}}{\rho_{k,n}})+\\&\mu(P^*-\sum_{k=1}^{K}\sum_{n=1}^{N}p_{k,n})+\beta_n(1-\sum_{k=1}^{K}\rho_{k,n}),\end{aligned} \tag{16}$$

where μ and $\beta_n,\forall n\in N$ are Lagrange multipliers corresponding to the transmission power constraint and the subcarrier constraints, respectively. Let $\mu^*,\beta_n^*,\forall n\in N$ denote the corresponding optimal Lagrange multipliers. Using the Karush-Kuhn-Tucker (KKT) conditions, we differentiate (16) with respect to $p_{k,n}$ and $\rho_{k,n}$, respectively. By setting each derivative to 0, (17) and (18) are obtained.

The optimal end-to-end transmission power $p_{k,n}^*$ on subcarrier n for user k can be derived from (17):

$$p_{k,n}^*=\Big[\frac{4\Phi_{k,n}(1-\theta^k)^2}{(\mu^*ln2(\sqrt{\Xi_{k,n}^2+\frac{8\Phi_{k,n}(1-\theta^k)}{\mu^*ln2}}-\Xi_{k,n}))^2}-\frac{\Psi_{k,n}^2}{4\Phi_{k,n}}\Big]^+, \tag{19}$$

where operation $[\cdot]^+$ denotes $[x]^+=max(0,x)$, $\Xi_{k,n}=\Psi_{k,n}-2\gamma_{RR,k,n}$. Accordingly, the optimal transmission power $p_{s,k,n}^*$ at the source and $p_{r,k,n}^*$ at the relay node are obtained by Lemma 1, and the optimal throughput $t_{k,n}^*$ is obtained by substituting $p_{k,n}^*$ into (13).

Also, the optimal subcarrier allocation indicator $\rho_{k,n}^*$ is obtained from (18). It can be known that subcarrier n should be assigned to user k satisfying

$$\rho_{k,n}^*=\begin{cases}1,k=k^*\\0,k\neq k^*,\end{cases} \tag{20}$$

where $k^*=\underset{k}{\mathrm{argmax}}(1-\theta^k)\big[log_2(1+\Lambda_{k,n}^*)-\frac{p_{k,n}^*\gamma_{SR,k,n}\gamma_{R\hat{D},k,n}}{ln(2)(1+\Lambda_{k,n}^*)}\frac{1}{\gamma_{RR,k,n}\Lambda_{k,n}^*+\Psi_{k,n}}\big]$, and $\Lambda_{k,n}^*$ is obtained by substituting $p_{k,n}^*$ into $\Lambda_{k,n}^*=\frac{\sqrt{4p_{k,n}^*\Phi_{k,n}+\Psi^2}-\Psi}{2\gamma_{RR,k,n}}$. Notice that multiplier $\beta_n,\forall n\in N$ is omitted due to subcarrier constraints being naturally satisfied by (20). Hence, the next aim is to determine the optimal Lagrange multiplier μ^* satisfying

$$\begin{aligned}&f(\mu)=P^*-\\&\sum_{k=1}^{K}\sum_{n=1}^{N}\Big[\frac{4\Phi_{k,n}(1-\theta^k)^2}{(\mu ln2(\sqrt{\Xi_{k,n}^2+\frac{8\Phi_{k,n}(1-\theta^k)}{\mu ln2}}-\Xi_{k,n}))^2}-\frac{\Psi_{k,n}^2}{4\Phi_{k,n}}\Big]^+\\&\quad=0.\end{aligned} \tag{21}$$

It can be found that (21) is a mono-increasing function for $\mu>0$, and $f(\mu)<0|_{\mu\to 0}$ and $f(\mu)>0|_{\mu\to+\infty}$. The searching upper bound can be set as $\mu_{upper}=max\{\frac{8\Phi_{k,n}}{ln(2)(\Psi_{k,n}-4\Xi_{k,n})}\},\forall k\in k,n\in N$.

Based on the theoretic analysis, we propose a so-called quasi-concave based FD EE-oriented resource allocation (Q-FERA) algorithm, summarized in Algorithm 1, to optimize the EE of the multiuser FD DF relaying system, under cross-layer constraints. The proposed Q-FERA algorithm presented in Subsection IV-B relies on finding P^*, which helps us transform the problem P3 into the problem P4. According to the characteristic of derivative, *i.e.,* $\frac{\partial\eta}{\partial P}\big|_{P^*}=\lim_{\Delta P\to 0}\frac{\eta(P^*+\Delta P)-\eta(P^*)}{\Delta P}$, P^* is readily obtained. The optimization results are summarized in TABLE I.

C. Properties of the EE-Oriented Resource Allocation

Based on the theoretic analysis above, some useful properties of the EE-oriented resource allocation are discovered.

Remark 1: Impact of transmission power on EE

In FD DF relaying system, EE shows a mono-increasing or quasi-concave shape with respect to the transmission power, as indicated by Theorem 1. Therefore higher transmission power does not ensure a higher EE. For the transmission power at the source $P_s=\sum_{k=1}^{K}\sum_{n=1}^{N}p_{s,k,n}$, the end-to-end capacity is non-decreasing with respect to P_s, and thus the assigned throughput is also non-decreasing with respect to P_s. However, EE may be degraded by the raised total power consumption. Differently, improving the transmission power at the relay $P_r=\sum_{k=1}^{K}\sum_{n=1}^{N}p_{r,k,n}$ may decrease both throughput and EE given a poor self-interference cancellation configuration.

$$\frac{\partial L}{\partial p_{k,n}}\bigg|_{\rho_{k,n}=\rho^*_{k,n}} = (1-\theta^k)\frac{\Phi_{k,n}}{ln(2)\sqrt{4p^*_{k,n}\Phi+\Psi^2_{k,n}}}\frac{2\rho^*_{k,n}}{2\rho^*_{k,n}\gamma_{RR,k,n}+\sqrt{4p^*_{k,n}\Phi+\Psi^2_{k,n}}-\Psi_{k,n}}-\mu^* = \begin{cases} <0, p^*_{k,n}=0 \\ =0, 0<p^*_{k,n}. \end{cases} \tag{17}$$

$$\begin{aligned}\frac{\partial L}{\partial \rho_{k,n}}\bigg|_{p_{k,n}=p^*_{k,n}} &= (1-\theta^k)log_2(1+\frac{\sqrt{4p^*_{k,n}\Phi+\Psi^2_{k,n}}-\Psi_{k,n}}{2\rho^*_{k,n}\gamma_{RR,k,n}})- \\ \frac{(1-\theta^k)}{ln(2)}&\frac{4p_{k,n}\Phi_{k,n}}{(2\rho^*_{k,n}\gamma_{RR,k,n}+\sqrt{4p^*_{k,n}\Phi+\Psi^2_{k,n}}-\Psi_{k,n})(\sqrt{4p^*_{k,n}\Phi+\Psi^2_{k,n}}+\Psi_{k,n})}-\beta^*_{k,n} = \begin{cases} <0, \rho^*_{k,n}=0 \\ \geq 0, \rho^*_{k,n}=1. \end{cases}\end{aligned} \tag{18}$$

TABLE I
SUMMARY OF OPTIMIZATION RESULTS

Parameters	Optimization Results
Subcarriers allocation policy $\rho^*_{k,n}$	Allocate subcarrier n to the user k satisfying $k^* = \underset{k}{\operatorname{argmax}}(1-\theta^k)\big[log_2(1+\Lambda^*_{k,n})-\frac{p^*_{k,n}\gamma_{SR,k,n}\gamma_{R\hat{D},k,n}}{ln(2)(1+\Lambda^*_{k,n})}\frac{1}{\gamma_{RR,k,n}\Lambda^*_{k,n}+\Psi_{k,n}}\big]$.
End-to-end power allocation policy $p^*_{k,n}$	$p^*_{k,n} = \Bigg[\frac{4\Phi_{k,n}(1-\theta^k)^2}{(\mu^* ln2(\sqrt{\Xi^2_{k,n}+\frac{8\Phi_{k,n}(1-\theta^k)}{\mu^* ln2}}-\Xi_{k,n}))^2}-\frac{\Psi^2_{k,n}}{4\Phi_{k,n}}\Bigg]^+$.
Power allocation policy $p^*_{r,k,n}$ at relay node	$p^*_{r,k,n} = \frac{\sqrt{4p^*_{k,n}\gamma_{SR,k,n}\gamma_{R\hat{D},k,n}\gamma_{RR,k,n}+(\gamma_{RR,k,n}+\gamma_{R\hat{D},k,n})^2}-(\gamma_{RR,k,n}+\gamma_{R\hat{D},k,n})}{2\gamma_{RR,k,n}\gamma_{R\hat{D},k,n}}$.
Power allocation policy $p^*_{s,k,n}$ at source	$p^*_{s,k,n} = p^*_{k,n} - p^*_{r,k,n}$.
Throughput assignment policy $t^*_{k,n}$	$t^*_{k,n} = log_2(1+\frac{\sqrt{4p^*_{k,n}\Phi_{k,n}+\Psi^2}-\Psi}{2\gamma_{RR,k,n}})$.
Lagrange multiplier μ^*	Obtained by solving equation (19) using bisection method, with the searching upper bound $\mu_{upper} = max\{\frac{8\Phi_{k,n}}{ln(2)(\Psi_{k,n}-4\Xi_{k,n})}\}, \forall k \in k, n \in N$.

As can be seen from (8), the signal transmitted from the relay is treated as self-interference to the relay's receiver. Therefore, higher transmission power P_r improves the power of self-interference with a poor self-interference cancellation. As a result, both throughput and EE are deteriorated.

There are other models that assume the residual self-interference only increases the noise power by a coefficient [16] or treat the residual self-interference as a noise-like constant (which are special cases of our generalized model). The residual self-interference in these models is independent of transmission power. Therefore, increasing transmission power P_r in this case guarantees a non-decreasing end-to-end throughput. However, EE may be degraded due to the increased transmission power. By replacing the residual self-interference in (13) as a noise-like constant, it is easy to prove that the EE is still mono-increasing or quasi-concave with respect to the transmission power.

Remark 2: EE-oriented water-filling for two-hop FD relaying system

By (20), it can be found that user k with lower $\gamma_{RR,k,n}$ has a higher opportunity to get subcarrier n, implying that it is preferable that a subcarrier be allocated to a user with less self-interference on that subcarrier. Similarly, it is obvious that more power will be allocated to subcarrier n with lower $\gamma_{RR,k,n}$ as shown in (19). It is different to the conventional water-filling algorithm in HD networks by taking the presence of residual self-interference and the channel conditions of links R-R, S-R and R-D into account, which can be classified as EE-oriented two-hop FD relaying water-filling policy.

Remark 3: Trade-off between EE and SE for two-hop FD relaying

For FD relaying with SE-oriented algorithms, the transmission power is fully utilized in the case of effective self-interference cancellation, where the power of the residual self-interference can be much lower than that of noise. However, the EE of SE-oriented FD relaying may be hindered by the incurred high total power consumption. Different from SE-oriented algorithms, FD relaying with EE-oriented algorithm makes trade-off between EE and SE, where the utilized transmission power may be lower than the available transmission power constraint. As a result, the total power consumption is lower than that of SE-oriented FD relaying, and higher EE can be obtained at the expense of SE.

Remark 4: Suitability of the Q-FERA for 60 GHz applications

With a fixed outage probability requirement, more aggressive throughput assignment matrix $\boldsymbol{T} = [t_{k,n}]_{K\times N}$ can be achieved with a higher Rician factor $\hat{k}$. Since cdf of chi-square

Algorithm 1 Quasi-concave based Full-Duplex Energy-Efficient Resource Allocation (Q-FERA) Algorithm

Input: $P_{max}, P_{c,sta}, P_{AD}, \omega, \varepsilon, \theta^k, h_{SR,k,n}, h_{RR,k,n}, l_{SR,k}, l_{RD,k}$ and $l_{RR,k}$, $\forall k \in K, n \in N$.

Output: Optimal subcarrier and end-to-end transmission power allocation policy $\boldsymbol{\rho}^*, \boldsymbol{P}^*$, and optimal throughput assignment policy $\boldsymbol{T}^*$.

1: Set $P = P_{max}$
2: **for** $n = 1 : N$ **do**
3:   **for** $k = 1 : K$ **do**
4:     Allocate subcarrier n the user k satisfying (20), calculate end-to-end transmission power $p_{k,n}$ according to (19) and assign throughput $t_{k,n}$ according to (13).
5:   **end for**
6: **end for**
7: Calculate $\frac{\partial \eta}{\partial P}$ at $P = P_{max}$.
8: **if** $\frac{\partial \eta}{\partial P}|_{P_{max}} \geq 0$ **then**
9:   **return** $P^* = P_{max}$, $\eta^* = \eta(\boldsymbol{\rho}^*, \boldsymbol{P}^*, \boldsymbol{T}^*)$
10: **else**
11:   Initialize the left bound $P_L = 0$, and the right bound $P_R = P_{max}$.
12:   **while** $|\frac{\partial \eta}{\partial P}|_{P_M}| < \delta$ (δ is a precision factor) **do**
13:     $P_M = \frac{P_L + P_R}{2}$.
14:     Do subcarrier and transmission power allocation policy and throughput assignment policy as did in steps $2-6$, with total end-to-end transmission power $P = P_M$ and $P = P_L$, respectively.
15:     **if** $\frac{\partial \eta}{\partial P}|_{P_L} \cdot \frac{\partial \eta}{\partial P}|_{P_M} \geq 0$ **then**
16:       $P_L = P_M$
17:     **else**
18:       $P_R = P_M$
19:     **end if**
20:   **end while**
21:   **return** $P^* = P_M$, $\eta^* = \eta(\boldsymbol{\rho}^*, \boldsymbol{P}^*, \boldsymbol{T}^*)$
22: **end if**

function $F(\cdot)$ is mono-decreasing with respect to its non-centrality parameter. Inversely, the inverse function $F^{-1}(\cdot)$ is mono-increasing with respect to its non-central parameter, which is $\frac{2|\widehat{h_{RD,k,n}}|^2}{\sigma^2_{error}}$ as derived. Higher Rician factor $\hat{k}$ leads to higher value of $\mathbb{E}\{|h_{RD,k,n}|^2\} = \mathbb{E}\{|\widehat{h_{RD,k,n}}|^2\}$ (assume the estimator is unbiased) and higher non-central parameter. As a result, higher throughput can be assigned while satisfying the target outage probability, and therefore higher EE is obtained.

The analysis above accords with intuition that, applying directional or narrow beam-width antenna provides strong LOS transmission and a higher Rician factor, *e.g.,* $\hat{k}$ ranges from $5-15$ dB in a typical 60 GHz indoor environment, where the channel is more flat with strong LOS components and poor NLOS components. In this case, more aggressive throughput assignment can be obtained while satisfying the outage probability naturally.

In some special scenarios, the channels at 60 GHz may follow Rayleigh distribution with the utilization of omnidirectional low gain antenna and long distance between transmitter and receiver [55]. By setting the Rician factor $\hat{k} = 0$, our algorithm is easily extended to a Rayleigh scenario. Also, the Saleh-Valenzuala (S-V) and two wave with diffuse power (TWDP) channels were modeled at 60 GHz in [48], which can actually be approximated as Rician distribution when $\hat{k} > 0$ and does not approach $+\infty$.

Remark 5: Impact of outage probability constraint on EE

Since capacity analysis does not capture the effect of outage with imperfect channel estimation, we introduce the definition of throughput and outage probability, which is constrained by θ^k. According to the theoretic analysis, the total average bits per second per Hz successfully delivered to users is given by $\sum_{k=1}^{K}(1-\theta^k)\sum_{n=1}^{N} t_{k,n}$ [56]. With a coarse outage constraint θ^k, the throughput arrangement $t_{k,n}$ can be aggressive. However, the term $(1-\theta^k)$ is degraded, indicating outage is more likely to occur. Inversely, with a stringent outage constraint θ^k, the term $(1-\theta^k)$ is improved and it is likely more data can be delivered to users successfully. However, a stringent outage constraint θ^k leads to a smaller value of $F^{-1}(\theta^k)$ and hence a conservative value of $t_{k,n}$ (see. (13)). Considering an extreme case that outage probability θ^k is an infinitely small value that approaches 0 ($\theta^k \to 0$). The first term $(1-\theta^k)$ is equal to 1, indicating all encoded information can be readily delivered to users without outage. However, the second term $t_{k,n}$ approaches 0 since the value of $\lim\limits_{\theta^k \to 0} F^{-1}(\theta^k)$ is equal to 0. Therefore, a stringent outage probability constraint does not necessarily guarantee higher EE or SE. Also, a coarse constraint may lead to poor EE.

TABLE II
ANALYTICAL COMPUTATIONAL COMPLEXITY (N: NUMBER OF SUBCARRIERS; K: NUMBER OF USERS; δ: REQUIRED PRECISION FACTOR IN ITERATIVE SEARCH; l_{ite}: NUMBER OF ITERATIONS[2])

Designs	Algorithms	Complexities
EE. Max	Q-FERA	$\mathcal{O}(2NKl_{ite1}) + l_{ite2}\mathcal{O}(4NKl_{ite1}) \approx \mathcal{O}(2NKl_{ite1})$.
	[3] QA-ERA in [25]	$\mathcal{O}(N(K+1)^3)log_2(\frac{1}{\delta})$
SE. Max	[4] FRAA in [16]	$\mathcal{O}(NKl_{ite3})log_2(\frac{1}{\delta})$
	[5] FDRA in [20]	$\mathcal{O}(NKl_{ite4})$

V. Complexity Analysis

In Section V, the complexity of the proposed algorithm is analyzed in terms of number of multiplications.

The Q-FERA algorithm is proposed to perform subcarrier allocation, transmission power allocation and throughput assignment jointly. At first, the gradient of EE is calculated at the maximum transmission power P_{max}, and the complexity

[2]The number of iteration l_{ite} depends on the number of multiplier variables in Lagrange function and the applied search algorithm, *i.e.,* ellipsoid searching is used in [25] while subgradient searching is used in [20].

[3]The QA-ERA algorithm in [25] is applied in LTE-based MIMO-OFDMA systems, which considers individual minimum throughput requirement for different users, which means more K multipliers needs to be found during iterations by the ellipsoid searching method.

[4]The FRAA algorithm in [16] is applied in FD OFDMA systems, and the local pareto optimality is used to solve the optimization problem.

[5]For fair comparison, the complexity of the algorithm in [20] is calculated in a simplified two-antenna infrastructure relay (one transmit antenna and one receive antenna at relay node) and single relay configuration.

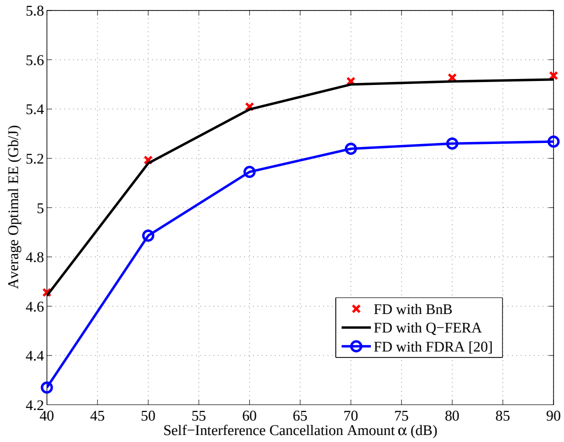

Fig. 2. The average EEs of FD with the BnB approach, FD with the Q-FERA and FD with the FDRA vs. different self-interference cancellation amounts.

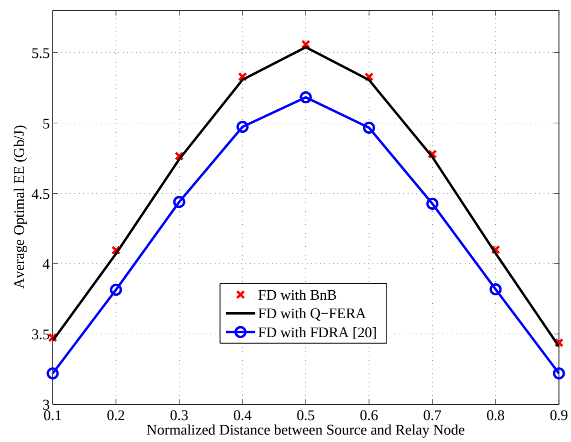

Fig. 3. The average EEs of FD with the BnB approach, FD with the Q-FERA and FD with the FDRA vs. different normalized distances between S-R, with self-interference cancellation amount $\alpha = 80$ dB.

of this step is $\mathcal{O}(2NKl_{ite1})$, where l_{ite1} is the number of iterations required to obtain the optimal Lagrange multiplier μ^* with given total transmission power P_{max}, and is upper bounded by $l_{ite1} \leq log_2(\frac{\mu_{upper}-\mu^*}{\delta})$ by bisection searching algorithm. The coefficient 2 is induced by the twice computation at the transmission power P_{max} and $P_{max}+\Delta P$, respectively. If $\frac{\partial \eta}{\partial P}|_{P_{max}} \geq 0$, $P_{max} = P^*$ is readily obtained and the algorithm terminates. Otherwise, the globally optimal transmission power P^* needs to be iteratively searched between (0, P_{max}], within at most $l_{ite2} \leq log_2(\frac{P_{max}-P^*}{\delta})$ iterations by bisection searching algorithm. Once the globally optimal transmission power P^* is found, the subcarrier and power allocation are allocated at the complexity $\mathcal{O}(4NKl_{ite1})$. Hence the total complexity of the whole algorithm is $\mathcal{O}(2NKl_{ite1}) + l_{ite2} \times \mathcal{O}(4NKl_{ite1})$.

Practically, the optimal transmission power always exists at the value that the transmission power related power consumptions (PA power P_{PA}, dynamic circuit power $P_{c,dyn}$) are comparable with the power consumption of the static power $P_{c,sta}$. Since the static power of 60 GHz chip is high while the feasible transmission power range is limited, *i.e.,* $P_{max} \leq 16$ dBm [57], P^* could be close to or even equal to P_{max}. Therefore, very few or no iteration l_{ite2} is needed in finding the optimal total transmission power P^*, and the whole complexity can be reduced to $\mathcal{O}(2NKl_{ite1})$ in this case. As a result, the complexity of the proposed Q-FERA is comparable with that of the SE-oriented algorithms in [16] and [20], and is lower than that of the EE-oriented algorithm in [25], which is for direct transmission rather than for relaying.

VI. SIMULATION RESULTS

We use numerical results to verify our analysis in Section VI. In all figures, we use Q-FERA to denote the proposed cross-layer EE-oriented resource allocation, and FD dynamic resource allocation (FDRA) to denote the SE-oriented resource allocation by the algorithm in [20]. The PL model in [2] is adopted, as $l = 68 + 10\nu log_{10}(d/d_0)$, where $\nu = 3$ is the PL exponent, d is the distance between two nodes, and $d_0 =$ 1 m is the reference distance. The Rician factor $\hat{k}$ is 15 dB except in Fig. 7. The total bandwidth is 2640 MHz with 512 subcarriers [58]. The AWGN power spectral density is -174 dBm/Hz. The S-R and R-D (all users and $K = 5$) distances are all 5 m. The drain efficiency ω of the PA is 25%. The static circuit power is 300 mW and the dynamic circuit factor $\varepsilon = 50$ mW/Gbps. The self-interference cancellation power is $P_{AD} = 40$ mW. The maximum transmission power constraint is set to $P_{max} = 50$ mW. The throughput outage constraint is $\theta^k = 0.01$ for all users, and the channel estimation error variance is set to $\sigma^2_{error} = 10^{-3}$ except in Fig. 6. To evaluate the optimality of the proposed Q-FERA algorithm, we adopt the brand-and-bound (BnB) approach [59] as a benchmark, which yields a theoretic optimum on subcarrier allocation.

Fig. 2 shows the average optimal EE performances of FD with different algorithms. It can be observed that FD with the Q-FERA algorithm shows higher EE than FD with the SE-oriented FDRA algorithm across a wide range of self-interference cancellation amount. The Q-FERA algorithm has nearly the same performance as the BnB approach, which certificates that our Q-FERA algorithm is near-optimal. Also, all the EEs of the FD systems increase with the self-interference cancellation amount, since less residual self-interference is left.

Fig. 3 demonstrates the average EEs of FD with different values of the normalized relay's position, which is defined as the ratio of the distance of S-R to the distance of S-D. Obviously, for all FD relaying curves, the optimal position of the FD relay is around in the middle between source and destinations. It is because with 80 dB of self-interference cancellation amount, the power of residual self-interference can be much smaller than the power of noise. The optimal EE performance is achieved when the throughputs of two links are equal. Besides, it can be seen that FD with the Q-FERA always outperforms FD with the FDRA in terms of EE at all distances. It indicates that FD relaying with the proposed Q-FERA algorithm maintains a high EE level. Last but not least, all the EE curves change rapidly with different relay's

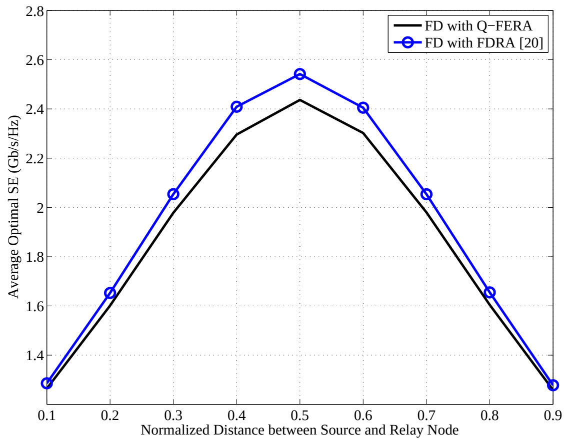

Fig. 4. The average SEs of FD with the Q-FERA and FD with the FDRA vs. different normalized distances between S-R, with self-interference cancellation amount $\alpha = 80$ dB.

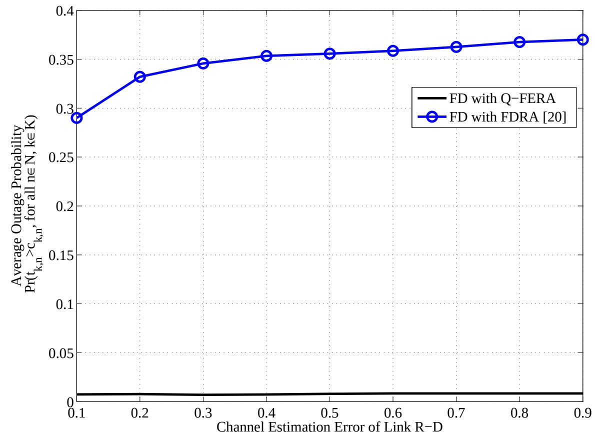

Fig. 6. The average outage probabilities that the assigned throughput is higher than channel capacity, *i.e.,* $\Pr(t_{k,n} > c_{k,n})$ for $\forall k \in K, n \in N$, under different channel estimation error, with self-interference cancellation amount $\alpha = 80$ dB.

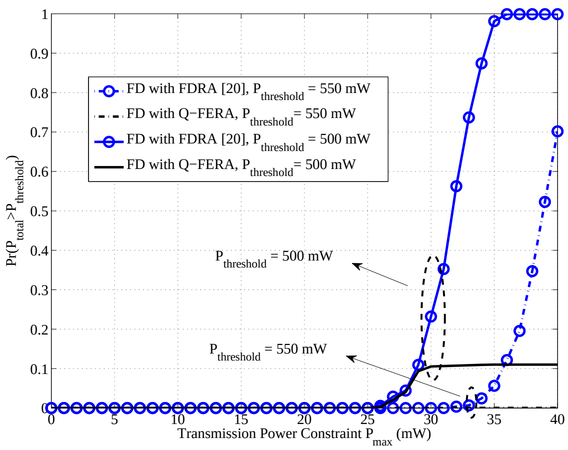

Fig. 5. The average probabilities that total power consumptions of FD with the Q-FERA and FD with the FDRA exceeds the thresholds $P_{threshold} =$ 500 mW and 550 mW, with self-interference cancellation amount $\alpha = 80$ dB.

position, since the high PL at 60 GHz results in a significant impact on system throughput.

Fig. 4 demonstrates the average SEs of FD with different values of the normalized relay's position. It shows that the EE-oriented Q-FERA algorithm offers a comparable SE to the SE-oriented FDRA algorithm. It means that FD with the proposed Q-FERA algorithm makes a proper trade-off between EE and SE, with marginal loss of SE.

Fig. 5 shows the probabilities that the total power consumption of FD relaying exceeds a threshold $P_{threshold}$. When P_{max} is lower than 25 mW, the probabilities of both the FD systems are equal to 0. With the increase of P_{max}, the outage probability of FD with the FDRA boosts fast, because the FDRA algorithm utilizes all available transmission power to maximize SE. Hence, its total power consumption easily exceeds the threshold of 500 mW (a reasonable power consumption of 60 GHz chips). While the probability of FD with the Q-FERA maintains low, which is only 0.1 with threshold 500 mW and $P_{max} \geq 30mW$. This indicates that to obtain higher EE performance, the utilized transmission power may be lower than the available transmission power constraint P_{max} and its EE may be quasi-concave with respect to the transmission power. Fig. 5 confirms that the proposed EE-oriented algorithm is a greener solution, with more carbon footprint savings.

Fig. 6 shows the average throughput outage probabilities of FD with the Q-FERA and FD with the FDRA. It can be observed that FD with the Q-FERA is robust against channel estimation errors, even though the system has no accurate channel information of the small-fading of the R-D link when $\sigma^2_{error} \rightarrow 1$ (which represents a noisy estimation in [49] [60]). This is because the channel condition of link R-D is adopted in a probabilistic manner in the proposed Q-FERA algorithm, as shown in Lemma 2. Therefore, the throughput outage probability is satisfied naturally in our cross-layer design. It is worth mentioning that the outage probability was not considered in the SE-oriented algorithm in [20], the throughput outage probabilities boosts with the increase of channel estimation error σ^2_{error}.

Fig. 7 shows the optimal average EEs of FD with the BnB approach, FD with the Q-FERA and FD with the FDRA under different Rician factors $\hat{k}$, whose value ranges from 5 dB to 15 dB in a typical indoor environment at 60 GHz. It is observed that higher Rician factor can improve the EEs of all FDs, since higher Rician factor means the R-D channel more flat with less fluctuation, and throughput can be assigned more aggressively while satisfying the preset outage probability. However, the EEs keep unchanged when the Rician factor is higher than 12 dB, this is because the LOS components almost overwhelm the NLOS components, and thus the channel is approximately a constant. Besides, it can be seen that FD with the Q-FERA (with $\alpha = 60$ dB) even shows higher EE than FD with the FDRA (with $\alpha = 80$ dB), which reflects that FD with the Q-FERA can maintain a considerable EE value

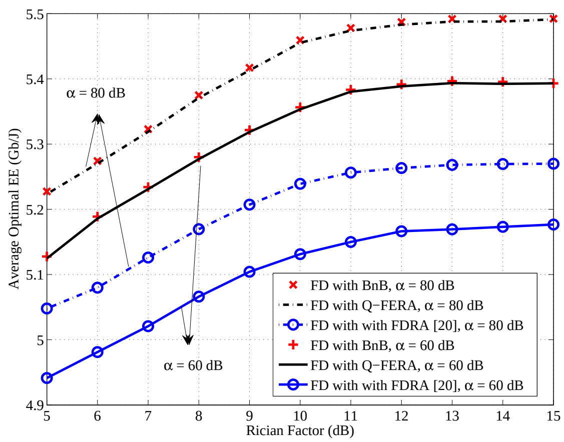

Fig. 7. The average EEs of FD with the BnB approach, FD with the Q-FERA and FD with the FDRA vs. different Rician factor $\hat{k}$, with self-interference cancellation amount α= 60 dB and 80 dB, respectively.

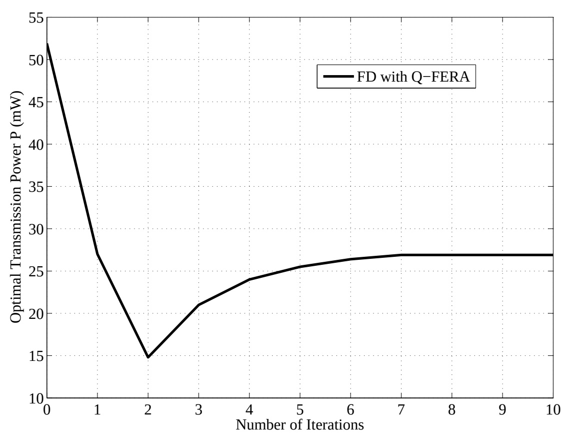

Fig. 8. The convergence behaviors of the proposed Q-FERA algorithm.

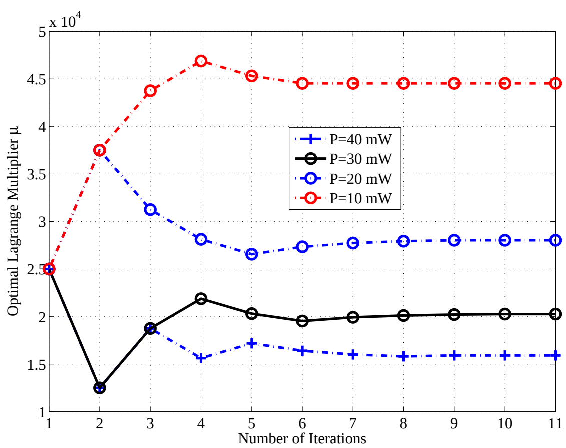

Fig. 9. The convergence behaviors of the proposed Q-FERA algorithm.

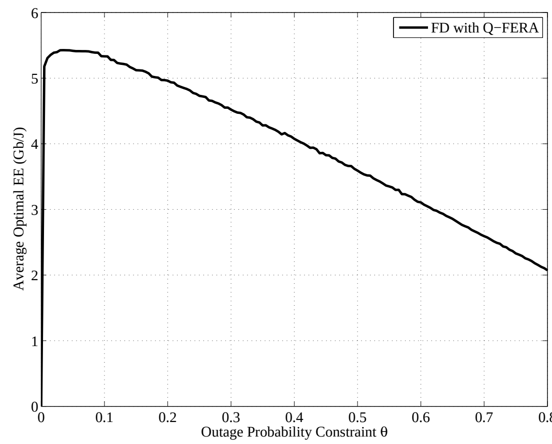

Fig. 10. The average EEs with different outage probability constraints, with cancellation amount α = 80 dB.

when self-interference cancellation performance is not very high, especially in a typically high Rician factor scenario at 60 GHz indoor environment.

Figs. 8 and 9 present the convergence behaviors of the Q-FERA algorithm under the maximum transmission power constraint P_{max} = 50 mW. Fig. 8 shows the convergence behavior of finding optimal transmission power P^*, while Fig. 9 shows the convergence behavior of finding the optimal multiplier μ^* with different values of given transmission power. It can be seen that the at most around 10 iterations are needed in both figures. Especially, if P_{max} is relatively small, EE may be mono-increasing in the range of $P_s \in (0, P_{max}]$, as analyzed in Theorem 1. In this case, the optimal transmission power P^* corresponding to the maximum EE is simply equal to P_{max}, and no iteration is needed in finding the optimal transmission power P^* in Fig. 8.

Fig. 10 presents the average EE performance with different outage probability constraints. It can be seen that EE approaches 0 given an infinitely small outage probability constraint, indicating a stringent outage probability constraint does not necessarily lead to better EE performance. Inversely, EE degrades significantly when constraint θ^k exceeds 0.1, which reveals that a coarse constraint may lead to poor EE and verifies Remark 5.

VII. Conclusion

In this paper, we have investigated EE-oriented resource allocation for indoor multiuser FD DF relay systems with cross-layer constraints. A novel low-complexity algorithm, referred to as Q-FERA, is proposed to perform transmission power allocation, subcarrier allocation and throughput assignment jointly to maximize system EE. Simulation results show a higher EE performance of the proposed EE-oriented design over SE-oriented design, at the cost of marginal SE loss. Also, the throughput outage probability of the proposed algorithm is much lower than that of the algorithm in [20] and is robust against channel estimation errors, addressing the intermittent blockage problem at mm-wave communications.

Besides, some useful properties of the EE-oriented resource allocation are discussed, such as the impact of transmission power on EE, EE-oriented water-filling power allocation, EE-SE trade-off for two-hop FD relaying system, the suitability of the Q-FERA algorithm for 60 GHz applications and the impact of outage probability constraint on EE. This work is extendable to a short-range wireless relaying system at a lower frequency.

APPENDIX A
DERIVATION OF LEMMA 2

Shannon capacity $c_{k,n}$ is the maximum rate of reliable communication supported by subcarrier n for user k. The quantity of $c_{k,n}$ is a function of the random channel gains and is therefore random. Suppose the source sends data at a rate $t_{k,n}$. If the arranged rate $t_{k,n}$ is higher than its upper bound $c_{k,n}$, then whatever code that was used by the transmitter, the decoding error probability cannot be made arbitrarily small. The transmission on subcarrier n is said to be in outage [60].

The outage probability in (C5) is equal to

$$\begin{aligned}&Pr[2\gamma_{RR,k,n}(2^{t_{k,n}-1}) > \\ &\quad\sqrt{4p_{k,n}\gamma_{SR,k,n}\gamma_{RD,k,n}\gamma_{RR,k,n}+(\gamma_{SR,k,n}+\gamma_{RD,k,n})^2} \\ &\quad-(\gamma_{SR,k,n}+\gamma_{RD,k,n}) \mid \hat{h_{RD,k,n}}]=\theta^k.\end{aligned} \tag{22}$$

The left hand of (22) can be re-sorted to

$$\begin{aligned}&Pr[\gamma_{RR,k,n}(2^{t_{k,n}}-1)^2+(2^{t_{k,n}}-1)\gamma_{SR,k,n} > \\ &\quad\gamma_{RD,k,n}(p_{k,n}\gamma_{SR,k,n}-(2^{t_{k,n}}-1)) \mid \hat{h_{RD,k,n}}].\end{aligned} \tag{23}$$

Note that since $p_{r,k,n}\gamma_{RR,kk,n} \geq 0$ and $p_{k,n}=p_{s,k,n}+p_{r,k,n}$, it can be derived that $log_2(1+\frac{p_{s,k,n}\gamma_{SR,k,n}}{1+p_{r,k,n}\gamma_{RR,k,n}}) \leq log_2(1+p_{k,n}\gamma_{SR,k,n})$. Since perfect CSI of link S-R is available at the source, $t_{k,n}$ will not exceed the real capacity of the S-R link as the corresponding perfect CSI is available at the scheduler, *i.e.*, $t_{k,n} \leq log_2(1+\frac{p_{s,k,n}\gamma_{SR,k,n}}{1+p_{r,k,n}\gamma_{RR,k,n}}) \leq log_2(1+p_{k,n}\gamma_{SR,k,n})$. Therefore, $2^{t_{k,n}}-1 < p_{k,n}\gamma_{SR,k,n}$ is readily obtained. Therefore, (23) is transformed into

$$\begin{aligned}&Pr\Bigg[|h_{RD,k,n}|^2 < \\ &\frac{(2^{t_{k,n}}-1)^2\gamma_{RR,k,n}+(2^{t_{k,n}}-1)\gamma_{SR,k,n}}{p_{k,n}\gamma_{SR,k,n}-(2^{t_{k,n}}-1)}\frac{\sigma^2}{l_{RD,k}} \mid \hat{h_{RD,k,n}}\Bigg].\end{aligned} \tag{24}$$

Since (24) is a conditional probability, we know the estimated channel $\hat{h_{RD,k,n}}$ and $h_{RD,k,n}=\hat{h_{RD,k,n}}+\Delta h_{RD,k,n}$. Therefore, (24) is equivalent to

$$\begin{aligned}&Pr\Bigg[|\hat{h_{RD,k,n}}+\Delta h_{RD,k,n}|^2 < \\ &\frac{(2^{t_{k,n}}-1)^2\gamma_{RR,k,n}+(2^{t_{k,n}-1})\gamma_{SR,k,n}}{p_{k,n}\gamma_{SR,k,n}-(2^{t_{k,n}}-1)}\frac{\sigma^2}{l_{RD,k}} \mid \hat{h_{RD,k,n}}\Bigg].\end{aligned} \tag{25}$$

(25) can be seen as the cdf of a non-central chi-square distributed variable. Substituting (25) into (22), we get

$$\begin{aligned}&F\bigg(\frac{(2^{t_{k,n}}-1)^2\gamma_{RR,k,n}+(2^{t_{k,n}}-1)\gamma_{SR,k,n}}{p_{k,n}\gamma_{SR,k,n}-(2^{t_{k,n}}-1)}\frac{2\sigma^2}{l_{RD,k}\sigma_{error}^2}\bigg) \\ &=\theta^k,\end{aligned} \tag{26}$$

where the operator $F(\cdot)$ denotes the cdf of the corresponding non-central chi-square function [49], with degree of freedom 2 and non-central parameter $\frac{2|\hat{h_{RD,k,n}}|^2}{\sigma_{error}^2}$ [56] [61]. Finally, (26) leads to Lemma 2.

The inverse function $F^{-1}(\cdot)$ is mono-increasing with respect to the non-central parameter, which is $\frac{2|\hat{h_{RD,k,n}}|^2}{\sigma_{error}^2}$ as derived. Hence, better channel estimation quality (smaller variance of channel estimation error σ_{error}^2) leads to more aggressive throughput assignment and higher EE with a given outage probability constraint. A similar impact of channel estimation error on system metrics can be found in [56] for CR networks.

APPENDIX B
PROOF OF THEOREM 1

For simplicity, let $T'=\sum_{k=1}^{K}(1-\theta^k)\sum_{n=1}^{N}\rho_{k,n}log_2(1+\frac{\Lambda_{k,n}}{\rho_{k,n}})$. Define the superlevel set of $\eta(\boldsymbol{P},\boldsymbol{\rho})$ is $S_\alpha=\{\boldsymbol{P}>0|\ \eta(\boldsymbol{P},\boldsymbol{\rho})>\alpha\}$. From [2], $\eta(\boldsymbol{P},\boldsymbol{\rho})$ is quasi-concave with respect to P if S_α is convex for any real number α. When α <0, there is no physical meaning. When $\alpha \geq$0, S_α is equivalent to $S_\alpha=\{P\geq 0|\frac{\alpha P}{\omega}+\alpha(P_{c,sta}+P_{AD})+(\alpha\varepsilon-1)T'\leq 0\}$. From [30], T' is strictly convex with respect to total transmission power P given a sufficiently large number of subcarriers. Besides, the linear part $\frac{\alpha P}{\omega}+\alpha(P_{c,sta}+P_{AD})$ is convex (not strictly) with respect to P. Therefore, the summation is strictly convex with respect to P. As a result, $\eta(\boldsymbol{P},\boldsymbol{\rho})$ is quasi-concave with respect to P.

APPENDIX C
PROOF OF CONCAVITY OF THE PROBLEM IN (15)

For the proof purpose, we first define a new variable $X_{k,n}=\sqrt{4p_{k,n}\Phi_{k,n}+\Psi_{k,n}^2}-\Psi_{k,n}$ for simplicity. The objective function is transformed to $u1(\rho_{k,n},X_{k,n})=\rho_{k,n}log_2(1+\frac{X_{k,n}-\Psi_{k,n}}{2\rho_{k,n}\gamma_{RR,k,n}})$. We first prove that the objective function is jointly-concave in terms of $\rho_{k,n}$ and $X_{k,n}$. The Hessian matrix of the objective is

$$\boldsymbol{H}(u1(\rho_{k,n},X_{k,n}))=\begin{pmatrix}\frac{-\rho_{k,n}}{ln(2)\varphi_{k,n}} & \frac{X_{k,n}-\Psi_{k,n}}{ln(2)\varphi_{k,n}} \\ \frac{X_{k,n}-\Psi_{k,n}}{ln(2)\varphi_{k,n}} & \frac{\frac{(X_{k,n}-\Psi_{k,n})^2}{\rho_{k,n}}}{ln(2)\varphi_{k,n}}\end{pmatrix}, \tag{27}$$

where $\varphi_{k,n}=(2\rho_{k,n}\gamma_{RR,k,n}+X_{k,n}-\Psi_{k,n})^2$. (27) can be further reduced to

$$\boldsymbol{H}(u1(\rho_{k,n},X_{k,n}))=\frac{X_{k,n}-\Psi_{k,n}}{ln(2)\varphi_{k,n}}\begin{pmatrix}\frac{-\rho_{k,n}}{X_{k,n}-\Psi_{k,n}} & 1 \\ 1 & \frac{X_{k,n}-\Psi_{k,n}}{-\rho_{k,n}}\end{pmatrix}. \tag{28}$$

It is straightforward (28) is a negative semi-definite matrix, indicating that $u1(\rho_{k,n}, X_{k,n})$ is jointly-concave in terms of $\rho_{k,n}$ and $X_{k,n}$.

Since $X_{k,n} = \sqrt{4p_{k,n}\Phi_{k,n} + \Psi_{k,n}^2} - \Psi_{k,n}$ is non-decreasing in terms of $p_{k,n}$, $u1(\rho_{k,n}, X_{k,n}) = \rho_{k,n}log_2(1 + \frac{X_{k,n}-\Psi_{k,n}}{2\rho_{k,n}\gamma_{RR,k,n}})$ is non-decreasing in terms of $p_{k,n}$. As a result, $u1(\rho_{k,n}, X_{k,n})$ is jointly-concave in terms of $\rho_{k,n}$ and $p_{k,n}$. Finally, it is easy to prove that $\sum_{k=1}^{K}(1-\theta^k)\sum_{n=1}^{N}\rho_{k,n}log_2(1+\frac{\Lambda_{k,n}}{\rho_{k,n}})$ is joint-concave in terms of $\rho_{k,n}$ and $p_{k,n}$.

References

[1] T. S. Rappaport *et al.,* "Millimeter wave mobile communications for 5G cellular: It will work!" *IEEE Access*, vol. 1, pp. 335-349, May 2013.

[2] Z. Wei, X. Zhu, S. Sun, Y. Huang, L. Dong and Y. Jiang, "Full-duplex vs. half-duplex amplify-and-forward relaying: which is more energy efficient in 60 GHz dual-hop indoor wireless systems?" *IEEE J. Sel. Areas Commun.*, vol. 33, no. 12, pp. 2936-2947, Dec. 2015.

[3] M. Duarte *et al.,* "Design and characterization of a full-duplex multi-antenna system for WiFi networks," *IEEE Trans. Veh. Tech.*, vol. 63, no. 3, pp. 1160-1177, Mar. 2014.

[4] K. Okada *et al.,* "Full four-channel 6.3-Gb/s 60-GHz CMOS transceiver with low-power analog and digital baseband circuitry," *IEEE J. Solid-State Circuit.*, vol. 48, no. 1, pp. 46-65, Jan. 2013.

[5] E. Everett, A, Sahai and A. Sabharwal, "Passive self-interference suppression for full-duplex infrastructure nodes," *IEEE Trans. Wireless Commun.*, vol. 13, no. 2, pp. 680-694, Feb. 2014.

[6] M. Jain *et al.,* "Practical, real-time, full duplex wireless," in *Proc. ACM MobiCom'10*, New York, USA, Sep. 2010, pp. 301-312.

[7] S. Huberman and T. L. Ngoc, "MIMO full-duplex precoding: a joint beamforming and self-interference cancellation structure," *IEEE Trans. Wireless Commun.*, vol. 14, no. 4, pp. 2205-2217, Apr. 2015.

[8] D. Bharadia, E. Mcmilim and S. Katti, "Full duplex radios," in *Proc. ACM SIGCOMM.*, Hong Kong, China, Aug. 2013, pp. 375-386.

[9] S. T. Choi, K. S. Yang, S. Nishi, S. Shimizu, K. Tokuda and Y. H. Kim, "A 60 GHz point-to-multipoint millimeter wave fiver-radio communication system," *IEEE Trans. Microw. Theory Tech.*, vol. 54, no. 5, pp. 1953-1960, May 2006.

[10] T. Dinc and H. Krishnaswamy, "A T/R antenna pair with polarization-based reconfigurable wideband self-interference cancellation for simultaneous transmit and receive," *in Proc. IEEE IMS'15*, Phoenix, USA, May. 2015, pp. 1-4.

[11] D. J. V. D. Broek, E. A. M. Klumperink and B. Nauta, "An in-band full-duplex radio receiver with a passive vector modulator down mixer for self-interference cancellation," *IEEE J. Solid-State Circuits.*, vol. 50, no. 12, pp. 3003-3014, Dec. 2015.

[12] L. Li, K. Josiam, R. Taori, "Feasibility study on full-duplex wireless millimeter-wave system," *in Proc. IEEE ICASSP'14*, Florence, Italy, May. 2014, pp. 2769-2773.

[13] V. V. Mai, J. Kim, S. W. Jeon, S. W. Choi, B. Seo and W. Y. Shin, "Degrees of freedom of millimeter wave full-duplex systems with partial CSIT," *to appear in IEEE Commun Lett*.

[14] A. C. Cirik, Y. Rong and Y. Hua, "Achievable rates of full-duplex MIMO radios in fast fading channels with imperfect channel estimation," *IEEE Trans. Signal Process.*, vol. 62, no. 15, pp. 3874-3886, Aug. 2014.

[15] D. Nguyen, L. N. Tran, P. Pirinen and M. Latvaaho, "On the spectral efficiency of full-duplex small cell wireless systems," *IEEE Trans. Wireless Commun.*, vol. 13, no. 9, pp. 4896-4910, Sep. 2014.

[16] C. Nam, C. Joo and S. Bahk, "Joint subcarrier assignment and power allocation in full-duplex OFDMA networks," *IEEE Trans. Wireless Commun.*, vol. 14, no. 6, pp. 3108-3119, Jun. 2015.

[17] H. Cui, M. Ma, L. Song and B. Jiao, "Relay selection for two-way full duplex relay networks with amplify-and-forward protocol," *IEEE Trans. Wireless Commun.*, vol. 13, no. 7, pp. 3768-3777, Jul. 2014.

[18] H. A. Suraweera, I. Krikidis, G. Zheng, C. Yuen and P. J. Smith, "Low-complexity end-to-end performance optimization in MIMO full-duplex relay system," *IEEE Trans. Wireless Commun.*, vol. 13, no. 2, pp. 913-927, Feb. 2014.

[19] T. Riihonen, S. Werner and R. Wichman, "Hybrid full-duplex/half-duplex relaying with transmit power adaptation," *IEEE Trans. Wireless Commun.*, vol. 10, no. 9, pp. 3074-3085, Sep. 2011.

[20] D. W. K. Ng, E. S. Lo and R. Schober, "Dynamic resource allocation in MIMO-OFDMA systems with full-duplex and hybrid relaying," *IEEE Trans. Commun.*, vol. 60, no. 5, pp. 1291-1304, May 2012.

[21] H. Kim, S, Lim, H. Wang and D. Hong, "Optimal power allocation and outage analysis for cognitive full duplex relay systems," *IEEE Trans. Wireless Commun.*, vol. 11, no. 10, pp. 3754-3765, Oct. 2012.

[22] C. Xiong, L. Lu and G. Y. Li, "Energy efficient spectrum access in cognitive radios," *IEEE J. Sel. Areas Commun.*, vol. 32, no. 2, pp. 550-562, Mar. 2014.

[23] J. Qiao, L. X. Cai, X. Shen, and J. W. Mark, "Enabling multi-hop concurrent transmissions in 60 GHz wireless personal area networks," *IEEE Trans. Wireless Commun.*, vol. 10, no. 11, pp. 3824-3833, Nov. 2011.

[24] C. W. Pyo and H. Harada, "Throughput analysis and improvement of hybrid multiple access in IEEE 802.15.3c mm-wave WPAN," *IEEE J. Select. Areas Commun.*, vol. 27, no. 8, pp. 1414-1424, Oct. 2009.

[25] X. Xiao, X. Tao and J. Lu, "Energy-efficient resource allocation in LTE-based mimo-ofdma systems with user rate constraints," *IEEE Trans. Veh. Tech.*, vol. 64, no. 1, pp. 185-197, Jan. 2015.

[26] L. Dong, S. Sun, X. Zhu and Y. K. Chia, "Power efficient 60 GHz wireless communication networks with relays," in *Proc. IEEE PIMRC'13*, London, UK, Sep. 2013, pp. 2808-2812.

[27] X. Hong, Y. Jie, C. Wang, J. Shi and X. Ge, "Energy-spectral efficiency trade-off in virtual MIMO cellular systems," *IEEE J. Sel. Areas Commun.*, vol. 31, no. 10, pp. 2128-2140, Oct. 2013.

[28] O. Waqar, M. A. Imran, M. Dianati and R. Tafazolli, "Energy consumption analysis and optimization of BER-constrained amplify-and-forward relay networks," *IEEE Trans. Veh. Tech.*, vol. 63, no. 3, pp. 1256-1269, Mar. 2014.

[29] X. Ge, X. Huang, Y. Wang, M. Chen, Q. Li, T. Han and C. Wang, "Energy-efficiency optimization for MIMO-OFDM mobile multimedia communication systems with QoS constraints," *IEEE Trans. Veh. Technol.*, vol. 63, no. 5, pp. 2127-2138, Jun. 2014.

[30] C. Xiong, G. Y. Li, S. Zhang, Y. Chen and S. Xu, "Energy-and spectral-efficiency tradeoff in downlink OFDMA networks," *IEEE Wireless Commun Lett.*, vol. 10, no. 11, pp. 3874-3886, Nov. 2011.

[31] C. Xiong, G. Y. Li, S. Zhang, Y. Chen and S. Xu, "Energy efficient resource allocation in OFDMA networks," *IEEE Trans. Commun.*, vol. 60, no. 12, pp. 3767-3778, Dec. 2012.

[32] C. Xiong, G. Y. Li, Y. Liu, Y. Chen and S. Xu, " Energy-efficient design for downlink OFDMA with delay-sensitive traffic," *IEEE Trans. Wireless Commun.*, vol. 12, no. 6, pp. 3085-3095, Jun. 2013.

[33] F. Haider, C. Wang, H. Haas, E. Hepsaydir, X. Ge and D. Yuan, "Spectral and energy efficiency analysis for cognitive radio networks," *IEEE Trans. Wireless Commun.*, vol. 14, no. 6, pp. 2969-2980, Jun. 2015.

[34] G. Yu, Q. Chen, R. Yin, H. Zhang and G. Y. Li, "Joint downlink and uplink resource allocation for energy-efficient carrier aggregation," *IEEE Trans. Wireless Commun.*, vol. 14, no. 6, pp. 3207-3218, Jun. 2015.

[35] G. Yu, Y. Jiang, L. Xu and G. Y. Li, "Multi-objective energy-efficient resource allocation for multi-rat heterogeneous networks," *IEEE J. Sel. Areas Commun.*, vol. 33, no. 10, pp. 2118-2127, Oct. 2015.

[36] F. Z. Kaddour, E. Vivier, L. Mroueh, M. Pischella and P. Martins, "Green opportunity and efficient resource block allocation algorithm for LTE uplink network," *IEEE Trans. Veh. Tech.*, vol. 64, no. 10, pp. 4537-4550, Oct. 2015.

[37] A. Aijaz, M. Tshangini, M. R. Nakhai, X. Chu and A. H. Aghvami, "Energy efficient uplink resource allocation in LTE networks with M2M/H2H co-existence under statistical QoS guarantees," *IEEE Trans. Commun.*, vol. 62, no. 7, pp. 2353-2365, Jul. 2014.

[38] F. D. Cardoso, S. Petersson, M. Blodi, S. Mizuta, G. Dietl, R. T. Duran, C. Desset, J. Leinonen and L. M. Correis, "Energy efficient transmission technique for LTE," *IEEE Commun. Mag.*, vol. 51, no. 10, pp. 182-190, Oct. 2013.

[39] G. Wu, C. Yang, S. Li and G. Y. Li, "Recent advances in energy-efficient networks and their application in 5G systems," *IEEE Wireless Commun.*, vol. 22, no. 2, pp. 145-151, Apr. 2016.

[40] Z. Gao, L. Dai, D. Mi, Z. Wang, M. A. Imran and M. Z. Shakir, "Mmwave massive-MIMO-based wireless backhaul for the 5G ultra-dense network," *IEEE Wireless Commun.*, vol. 22, no. 5, pp. 13-21, Oct. 2015.

[41] X. Ge, S. Tu, G. Mao, C. Wang and T. Han, "5G ultra-dense cellular networks," *IEEE Wireless Commun.*, vol. 23, no. 1, pp. 72-79, Feb. 2016.

[42] X. Ge, J. Ye, Y. Yang and Q. Li, "User mobility evaluation for 5G small cell networks based on individual mobility model," *IEEE J. Sel. Areas Commun.*, vol. 34, no. 3, pp. 528-541, Mar. 2016.

[43] G. Liu, F. R. Yu, H. Ji and V. C. M. Leung, "Energy-efficient resource allocation in cellular networks with shared full-duplex relaying," *IEEE Trans. Veh. Technol.*, vol. 64, no. 8, pp. 3711-3724, Aug. 2015.

[44] L. J. Rodriguez, N. H. Tran, and T. L. Ngoc,"Performance of full-duplex AR relaying in the presence of residual self-interference," *IEEE J. Sel. Areas Commun.*, vol. 32, no. 9, pp. 1752-1764, Sep. 2014.

[45] S. Geng, J. Kivinen, X. Zhao and P. Vainikainen, "Millimeter-wave propagation channel characterization for short-range wireless communications," *IEEE Trans. Wireless Commun.*, vol. 58, no. 1, pp. 3-12, Jan. 2009.

[46] D. Dardari and V. Tralli, "High-speed indoor wireless communications at 60 GHz with coded OFDM," *IEEE Trans. Commun.*, vol. 47, no. 11, pp. 1709-1721, Nov. 1999.

[47] N. Moraitis and P. Constantinou, "Measurements and characterization of wideband indoor radio channel at 60 GHz," *IEEE Trans. Commun.*, vol. 5, no. 4, pp. 880–889, Apr. 2006.

[48] T. S. Rappaport, R. W. Heath, R. C. Daniels and J. N. Murdock, "Millimeter wave wireless communications," *Prentice Hall*, 2015.

[49] D. W. K. Ng and R. Schober, "Cross-layer scheduling for OFDMA amplify and forward relay networks," *IEEE Trans. Veh. Tech.*, vol. 59, no. 3, pp. 1443-1458, Mar. 2010.

[50] K. Dong, X. Liao and S. Zhu, "Link blockage analysis for indoor 60 GHz radio system," *IET Electron. Lett.*, vol. 48, no. 23, pp. 129-130, Nov. 2012.

[51] G. Caire, G. Taricco and E. Biglieri, "Optimum power control over fading channels," *IEEE Trans. Inf. Theory.*, vol. 45, no. 5, pp. 1468-1489, Jun. 1999.

[52] D. V. Hoang, V. Subramanian, W. Keusgen and G. Boeck, "A 60 GHz SiGe-HBT power amplifier with 20% PAE at 15 dBm output power," *IEEE Microw. Wireless Compon.*, vol. 18, no. 3, pp. 209-211, Mar. 2008.

[53] W. Yu and R. Lui, "Dual methods for nonconvex spectrum optimization of multicarrier systems," *IEEE Trans. Commun.*, vol. 54, no. 7, pp. 1310-1322, Jul. 2006.

[54] N. Zhou, X. Zhu and Y. Huang, "Optimal asymmetric resource allocation and analysis for OFDM-based multidestination relay systems in the downlink," *IEEE Trans. Veh. Tech.*, vol. 60, no. 3, pp. 1307-1312, Mar. 2011.

[55] T. Zwick, T. J. Beukema and H. Nam, "Wideband channel sounder with measurement and model for the 60 GHz indoor radio channel," *IEEE Trans. Veh. Tech.*, vol. 54, no. 3, pp. 1266-1277, Jul. 2005.

[56] M. Mallick, R, Devarajan, R. A. Loodaricheh and V. K. Bhargava, "Robust resource allocation optimization for cooperative cognitive radio networks with imperfect CSI," *IEEE Trans. Wireless Commun.*, vol. 14, no. 2, pp. 907-920, Feb. 2015.

[57] C. Marcu *et al.,* "A 90 nm CMOS low-power 60 GHz transceiver with integrated baseband circuitry," *IEEE J. Solid-State Circuit.*, vol. 44, no. 12, pp. 3434-3447, Dec. 2009.

[58] (15 Mar. 2014) Enhancements for very high throughput in the 60 GHz band (adoption of IEEE Std 802.11ad-2012) [Online]. Available:http://www.iso.org/iso/catalogue_detail.htm?csnumber=64876.

[59] Y. Lin, T. Chiu and Y. T. Su, "Optimal and near-optimal resource allocation algorithm for OFDMA networks," *IEEE Trans. Wireless Commun.*, vol. 8, no. 8, pp. 4066-4077, Aug. 2009.

[60] D. Tse and P. Viswanath, "Fundamentals of wireless communications," *Cambridge University Press*, 2005.

[61] M. Mallick, R, Devarajan, M. M. Rashid and V. K. Bhargava, "Resource allocation for selective relaying based celluar wireless system with imperfect CSI," *IEEE Trans. Commun.*, vol. 61, no. 5, pp. 1822-1834, May 2013.

Zhongxiang Wei (S'15) received the M.S. degree in 2013, in Information and Communication Engineering from Chongqing University of Posts and Telecommunications, Chongqing, China. He is currently a Ph.D. candidate at the Department of Electrical Engineering and Electronics, the University of Liverpool. His research interests include green communications, full-duplex, millimeter-wave communications, wireless resource allocation and algorithm design.

Xu Zhu (S'02-M'03-SM'12) received the BEng degree (with the first class honors) in Electronics and Information Engineering from Huazhong University of Science and Technology, Wuhan, China, in 1999, and the PhD degree in Electrical and Electronic Engineering from the Hong Kong University of Science and Technology, Hong Kong, in 2003. Since 2003, she has been with the Department of Electrical Engineering and Electronics, the University of Liverpool, Liverpool, UK, where she is currently a Reader. Dr. Zhu has over 140 peer-reviewed publications on communications and signal processing. She is an Editor for the IEEE Transactions on Wireless Communications, and has served as a Guest Editor for several international journals. She was Symposium Co-Chair of the IEEE ICC 2016, Vice Chair of the 2006 and 2008 ICARN International Workshops, Program Chair of the ICSAI 2012, and Publication Chair of the IEEE IUCC-2012 and IUCC-2014. Her research interests include MIMO, equalization, resource allocation, cognitive radio, smart grid communications *etc*.

Sumei Sun (Fellow'16) is Head of the Cognitive Communications Technology Department, Institute for Infocomm Research, Agency for Science, Technology, and Research, Singapore. Her research focus is energy- and spectrum-efficient communication technologies for connecting human, machines, and things. Dr Sun is inventor and co-inventor of thirty granted patents and more than thirty pending patent applications, many of which have been licensed to industry. She has authored and co-authored more than two hundred technical papers in prestigious IEEE journals and conferences. She has also been actively contributing to organizing conferences in different roles. Some of her recent conference services include Executive Vice Chair of Globecom 2017, Symposium Co-Chair of ICC 2015 and 2016, Track Co-Chair of IEEE VTC 2012 Spring, VTC 2014 Spring and VTC 2016 Fall, Publicity Co-Chair of PIMRC 2015, *etc*. She is an Editor for IEEE Transactions on Vehicular Technology (TVT) since 2011, Editor for IEEE Wireless Communication Letters during 2011-2016, and Editor of IEEE Communications Surveys and Tutorials since 2015. She received the "Top Editor Award" in 2016, Top15 Outstanding Editors recognition in 2014, and "Top Associate Editor" recognition in 2013 and 2012, all from TVT. She is a distinguished lecturer of IEEE Vehicular Technology Society 2014-2016, a co-recipient of the 16th PIMRC Best Paper Award, and Distinguished Visiting Fellow of the Royal Academy of Engineering, UK, in 2014.

Yi Huang (S'91-M'96-SM'06) received the DPhil in Communications from the University of Oxford, UK in 1994. He has been conducting research in wireless communications, applied electromagnetics, radar and antennas since 1987. His experience includes 3 years spent with NRIET (China) as a Radar Engineer and various periods with the Universities of Birmingham, Oxford, and Essex at the UK. He worked as a Research Fellow at British Telecom Labs in 1994, and then joined the University of Liverpool, UK in 1995, where he is now a full Professor and Deputy Head of the Department of Electrical Engineering and Electronics. Dr. Huang has published over 300 refereed papers, received many research grants from various funding bodies and acted as consultant for various companies. He has been a keynote/invited speaker and organizer of many conferences and workshops (*e.g.*, WiCom2010, IEEE iWAT 2010 and LAPC2012). He is the Editor-in-Chief of Wireless Engineering and Technology and has been an Editor or Guest Editor for four international journals. He is a UK national representative of EU COST-IC1102 and Executive Committee Member and Fellow of the IET.